CONF-9508145--

BNL-61945

Phase transformation and phonon anomalies in Ni_2MnGa.

*A. Zheludev**, *S. M. Shapiro and P. Wochner*
Brookhaven National Laboratory, Upton, New York 11973-5000.

A. Schwartz, M. Wall and L. E. Tanner
Lawrence Livermore National Laboratory, Livermore, California 94550.

* Physics Department, bld. 510B, Brookhaven National Lab, P.O. Box 5000, Upton, NY11973-5000.
Tel: (516) 282 3734 Fax: (516) 282 2918 e@mail: zhelud@solids.phy.bnl.gov

A. Zheludev

Abstract. Inelastic neutron scattering experiments and transmission electron microscopy have been used to study a single crystal of the Ni_2MnGa shape memory Heusler alloy in a wide temperature range covering the parent phase ($T>T_1$=265 K), a recently discovered premartensitic ($T_1>T>T_M$)and martensitic ($T<T_M$=220 K) phase regions. A temperature- dependent anomaly in the TA_2 phonon dispersion in the parent phase was observed and related to the phase transformations. The premartensitic phase involves a transverse modulation of the parent cubic structure with a simple periodicity of 1/3 [1 1 0]. The approximately tetragonal lattice of the low-temperature martensite is distorted by transverse modulations with incommensurate wave vectors [ζ_M ζ_M 0] and [$2\zeta_M$ $2\zeta_M$ 0], $\zeta_M \approx 0.43$. The observed phenomena are attributed to electron-phonon interactions and anharmonic effects.

1. INTRODUCTION.

The Ni2MnGa Heusler alloy is an interesting model system for studying martensitic transformations (MT's) and premartensitic (PM) phenomena. This material combines bulk ferromagnetism ($T_C \approx 380$ K) with shape memory behavior and a MT at $T_M \approx 220$ K. A number of thermally- and stress- induced martensites have been observed in this compound [1,2]. Thermal diffuse X-ray scattering experiments [3] suggested the transformation is associated with a soft transverse acoustic (TA) phonon with the wave vector [ζ ζ 0] and polarization along [1 $\bar{1}$ 0] (the so-called TA_2, or Zener mode) in the high-temperature cubic (parent) phase. In the present paper we report the results of our inelastic neutron scattering, neutron diffraction and electron microscopy/ diffraction studies of the precursor effects in the parent phase. In addition, we identify a new thermally-induced premartensitic transition, which occurs at $T_1 \approx 265$ K. Finally, neutron diffraction experiments allow us to determine the structure of the low-temperature martensite, which appears to be tetragonal on the average, but incommensurably modulated along the (1 $\bar{1}$ 0) directions.

2. EXPERIMENTAL.

At room temperature Ni_2MnGa has a f.c.c. $L2_1$ Heusler structure (space group Fm3m, no.225), the cell constant being 5.822Å [1]. The structure can be viewed as being composed of eight b.c.c. units ($a_{b.c.c.}=1/2\ a_{f.c.c.}$), with Ni at the cube center and Mn and Ga at the corners. Three types of Bragg reflections exist: the order-independent principal b.c.c. reflections with $h+k+l=4n$; reflections of type $h+k+l=4n+2$, corresponding to a B2 (CsCl- type) structure; and the weaker superlattice reflections with h,k,l all odd. The use of b.c.c. indexing may be sometimes found in literature, but for the sake of clarity the correct f.c.c. notation will be used throughout this paper.

A large (70×15×10 mm^3) single crystal sample was grown by Brigdman method at Ames Laboratory particularly for these experiments. The martensitic phase transition temperature $T_M \approx 220$ K was estimated from the splitting of the [2 2 0] Bragg peak which occurs at 212 K on cooling and 228 K on warming up, thus showing a significant temperature histeresis. The MT was found to be completely reversible. As will be discussed in detail below, the low- temperature martensitic structure is roughly tetragonal with a complex [1 1 0]-transverse modulation along the [1 $\bar{1}$0] directions [2].

Neutron scattering experiments were carried out on the H4M and H8 triple axis spectrometers at the HFBR at Brookhaven National Laboratory. The use of standard and high-temperature Displex

refrigerators enabled us to perform the measurements over a wide temperature range 12-400 K. Two sample settings were used. The crystal was aligned to have either the (1 0 0) or the (110) planes coincide with the scattering plane of the spectrometer. The sample mosaic reveals two monocrystalline grains, misaligned by 0.5°, giving a total Bragg FWHM of 1°. Neutron scattering experiments were performed with fixed final or initial neutron energies, E=14.7 meV and E=30.5 meV. Pyrolitic graphite PG(002) reflections were used for monochromator and analyzer. A typical 20'-20'-20'-40' setup provided an energy resolution of δE=0.4 meV FWHM at ΔE=0, E_f=14.7 meV. A pyrolitic graphite filter was positioned in front of the detector or in front of the sample for E_f-constant and E_i-constant measurements, respectively.

Conventional electron microimages (amplitude contrast) and selected-area electron diffraction (SAED) patterns were obtained with the standard JEOL 200 CX instrument equipped with double-tilt heating and cooling stages at Lawrence Livermore National Laboratory. High-resolution imaging (phase contrast), which is limited to room temperature, was carried out on the JEOL top-entry 200 CX and ARM instruments at the National Center for Electron Microscopy at the Lawrence Berkeley Laboratory.

3. RESULTS.

3.1. Precursor phenomena in the parent phase.

3.1.1. Phonon dispersion.

Phonon dispersion curves were determined from inelastic neutron scattering along the high-symmetry directions [ζ 0 0], [ζ ζ 0], [ζ ζ ζ] and [2ζ ζ ζ] using constant-q and constant-E scans. The results are shown in Fig. 1. The curves are plotted in an extended Brillouin zone scheme of the f.c.c. $L2_1$ structure.

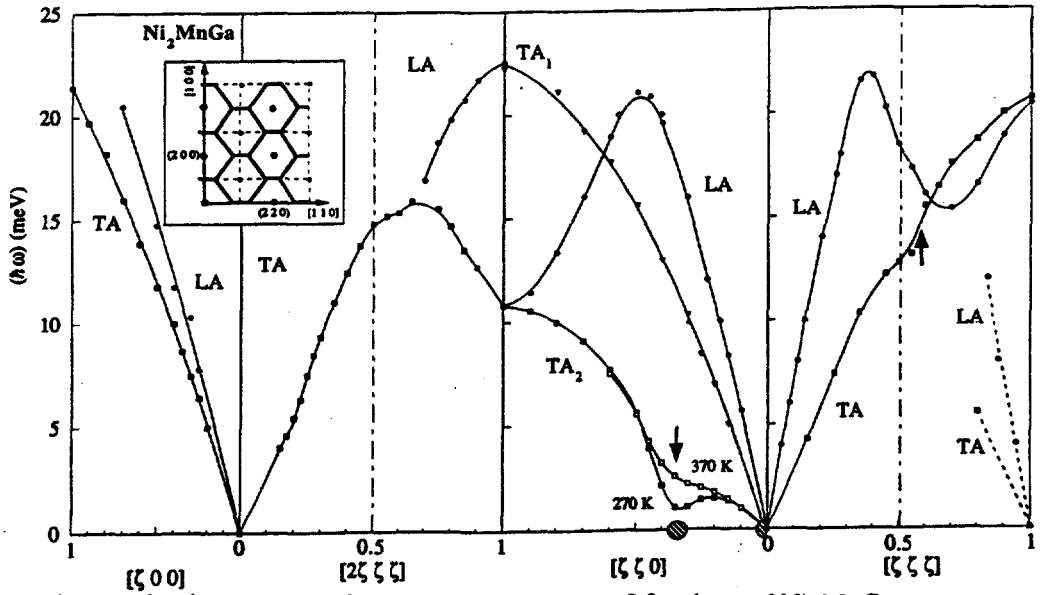

Figure 1: Measured acoustic-phonon dispersion curves for the parent $L2_1$ phase of Ni_2MnGa.

Most modes demonstrate only slight temperature dependence easily explained by the overall stiffening of the lattice at low temperatures. The most striking feature, however, is the strong temperature dependence of the [ζ ζ 0] (1 $\bar{1}$ 0) TA_2 branch. As shown in the blowup in Fig. 2(a), the dispersion curve has a wiggle at $\zeta_0 \approx 1/3$ at room temperature, which develops into a distinct minimum as the temperature is decreased. The softening of the TA_2 phonon is incomplete, though a threefold reduction of its frequency is observed on cooling from 400 to 260 K. In the limit $\zeta \rightarrow 0$ the [ζ ζ 0] TA_2 mode corresponds to the Zener elastic constant $c'=1/2(c11-c12)$, which is known to be reduced in b.c.c. materials, and shows an anomalous decrease as $T \rightarrow T_M$ in Ni_2MnGa [4].

Figure 2(b) shows a plot of the phonon energy measured in a perpendicular [1 $\bar{1}$ 0] direction from the q=1/3 [1 1 0] point, where the phonon energy is a minimum. The phonon energy increases dramatically, as the wave vector deviates from the [1 1 0] direction. Thus the anomaly in the dispersion manifold is restricted to a narrow valley along [1 1 0].

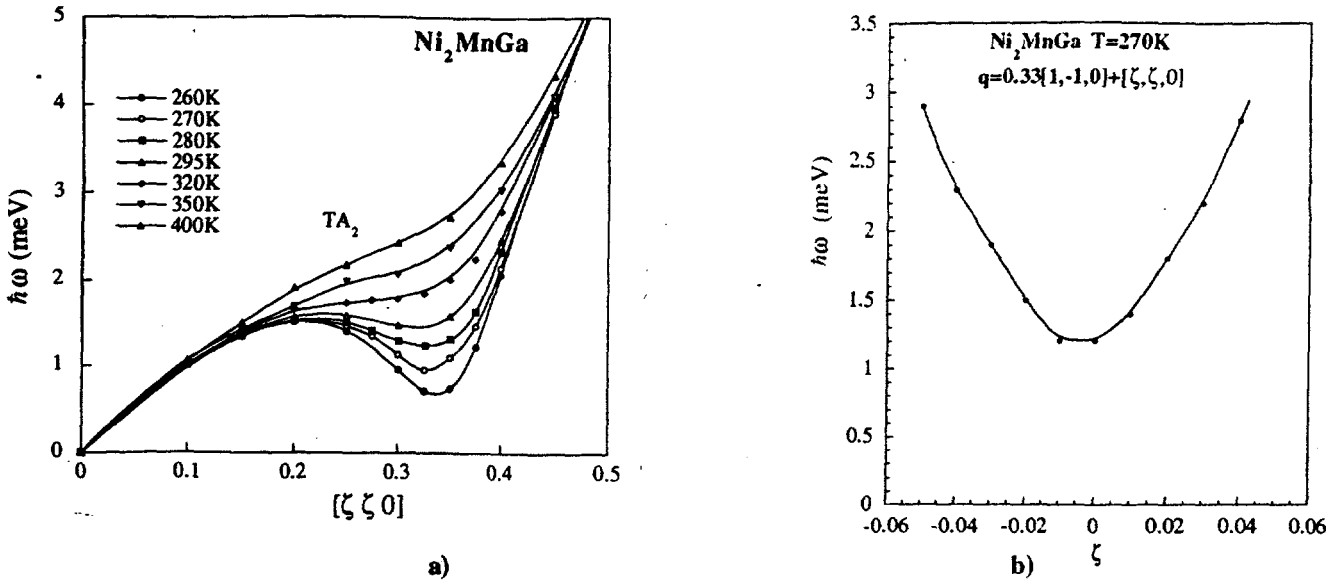

Figure 2: Temperature dependence of the phonon anomaly in the [ζ ζ 0] TA2 branch (a). Phonon energies measured in a perpendicular [ζ ζ 0] direction from the q=1/3 [1 $\bar{1}$ 0] point (b).

3.1.2. Quasielastic scattering.

Associated with the dip in the [ζ ζ 0] TA2 phonon dispersion curve is a quasielastic diffuse "central peak", which shows up in [ζ ζ 0] transverse scans in the vicinity of 1/3[1 1 0] Fig. 3(a). Its intensity increases steadily as the frequency of the corresponding TA2 phonon decreases. Its shape in *q*-space *roughly coincides with that of the dip in the dispersion manifold* and its *q*-width is *T*-independent (Δq 0.15Å^{-1}) at $T>T_1$. The energy width of the peak is resolution-limited. Just like the phonon anomaly, it is localized in a narrow valley along [1 1 0]. All this suggests that the diffuse peak is defect- induced and is directly related to the reduction of vibrational frequencies as explained by the model proposed by Axe *et al* [5] and Halperin and Varma [6].

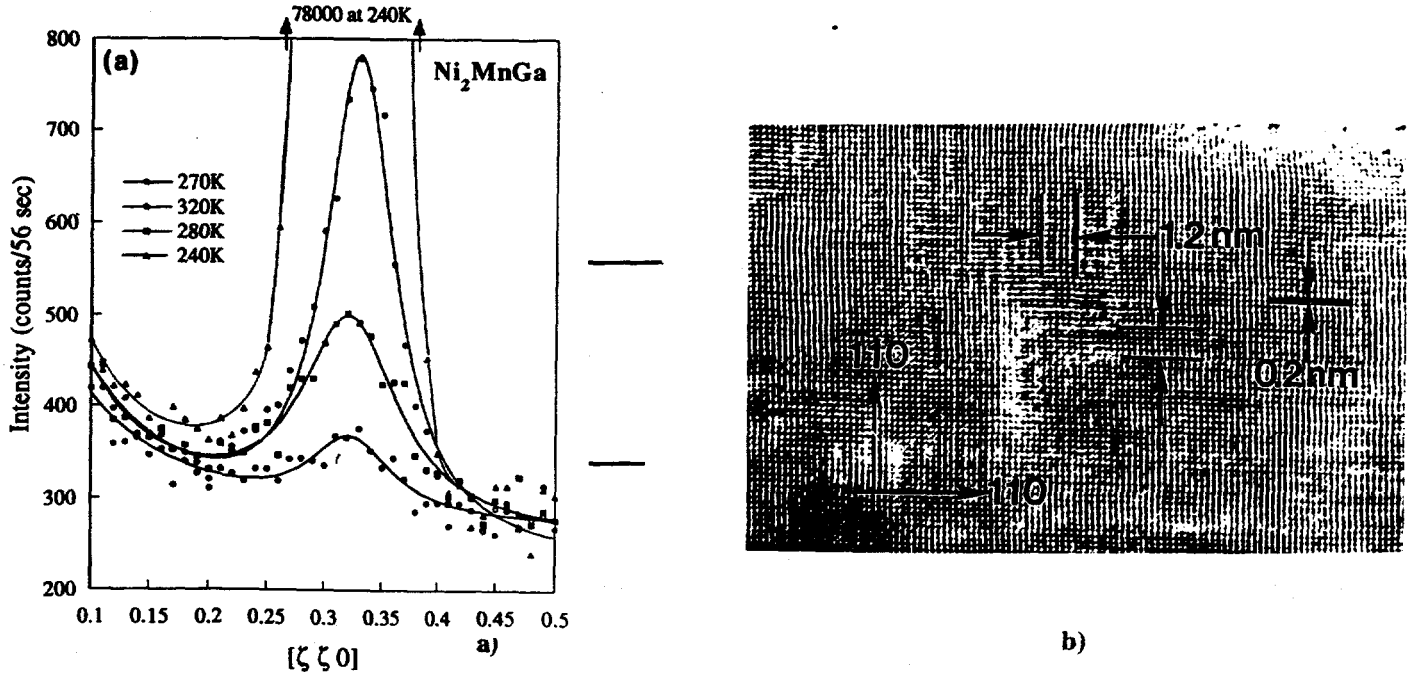

Figure 3: Elastic scattering in the [ζ ζ 0] (transverse) direction measured at different temperatures (a). HRTEM micro structural images showing local atomic displacements and micromodulated domain structure of the parent phase (b).

3.1.3. Electron microimaging.

The microstructure related to the [1/3 1/3 0] satellites can be directly observed by high-resolution, multi-beam phase contrast imaging (HRTEM) [7] and these local atomic configurations are seen in Fig. 3(b). The normal (unstrained) image of the $L2_1$ structure in this orientation is a square pattern of sharply aligned white dots corresponding to atomic columns lying in (2 2 0) planes. We see that this pattern is severely perturbed. The result is an inhomogeneous assembly of contiguous distorted regions of roughly 4-6 nm extent (this corresponds to the observed q-width of the elastic satellites). Each region consists of alternating dark/light bands of approximately 1.2 nm width parallel to either the (2 2 0) or (2 2 0) planes (*viz.*, a quasi-periodicity of six (2 2 0) planes). This band width is the inverse of the satellite spacings found in reciprocal space.

3.2. The premartensitic transition.

The progressive softening of TA_2 phonons propagating in the [1 1 0] direction leads to a PM phase transition at T_1=260 K. The first indication to the existence of this phase was obtained in magnetoelastic measurements[8]. Though the PM transition, unlike the MT at a lower temperature, does not manifest itself in the magnetic susceptibility [1], magnetostriction shows a distinct kink at T_1.

The most direct evidence for the existence of the PM phase is the behavior of the [1/3 1/3 0] (transverse) elastic satellite. At higher temperatures the peak is broad and relatively weak (Fig. 4a). As the temperature decreases below T_1 it becomes narrow and Bragg-like (Fig. 4b,c). Its intensity increases dramatically and its q-width becomes defined by the crystal mosaic spread, rather than the shape of the dip in the phonon dispersion curve.

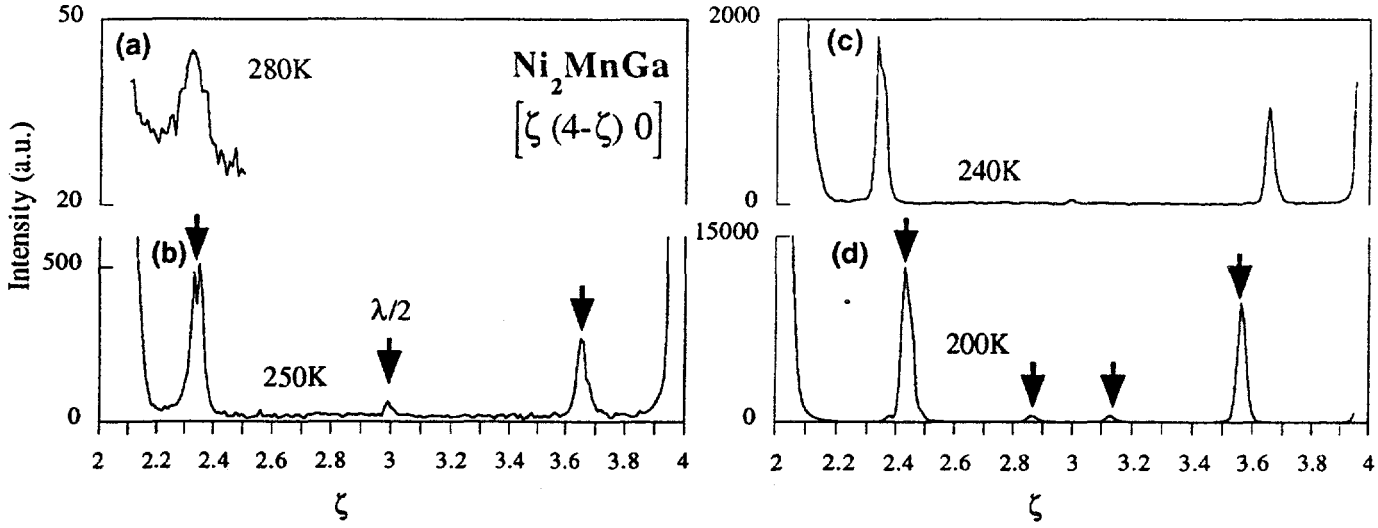

Figure 4: Elastic scattering along the [ζ ζ 0] (transverse) direction in the parent (a), premartensitic (b, c) and martensitic (d) phases of Ni_2MnGa.

It could be expected that the formation of the PM phase, which is characterized by a new [1/3 1/3 0] transverse modulation of the parent cubic structure, should be accompanied by a uniform distortion of the latter. Experimentally, this has not been observed: neither splitting nor shifting of the original f.c.c. Bragg peaks were detected below T_1. Only their intensity was found to decrease slightly.

Characteristic of the PM phase is the *stiffening* of the TA_2 phonon with decreasing temperature. This is borne out in Fig. 5. The fact that the phonon softening is *incomplete* suggests that the phase transformation in Ni_2MnGa at T_1 is of the first order and is not a Cochran-Anderson "frozen phonon" transition of the type seen in materials like $SrTiO_3$ [9].

3.3. The low-temperature martensite.

As the temperature is further lowered below T_M, the actual martensitic transformation occurs, which involves *both* a periodic modulation and a strong tetragonal distortion of the lattice. Relying on the results of X-ray diffraction experiments, Martynov and Kokorin [2] suggested that the martensitic phase is approximately tetragonal with $a=b=5.90$ Å, $c=5.54$ Å, $c/a=0.94$, modulated along $[\zeta_M\ \zeta_M\ 0]$, $\zeta_M=0.4$ with displacements along $[1\ \bar{1}\ 0]$ (5-layer (2 2 0)- plane martensite). This implies that in a transverse elastic scan from $[2\ 2\ 0]_{tetr.}$ to $[4\ 0\ 0]_{tetr.}$ four equally spaced superstructure Bragg peaks should appear. Our experiments (Fig. 4d) show that the behavior of our samples different. Indeed, four peaks are observed, but they are *not* equally spaced. Their positions $[\zeta_M\ \zeta_M\ 0]$ and $[2\zeta_M\ 2\zeta_M\ 0]$, $\zeta_M=0.43$, found to be the same in different Brillouin zones, correspond to an incommensurate modulation of the average tetragonal structure along the $[1\ 1\ 0]_{tetr.}$ direction with displacements along $[1\ 1\ 0]_{tetr.}$. Such a periodicity is *substantially different from the one observed in the PM phase*, where the modulation occurs with $\zeta_0=0.33$.

4. DISCUSSION.

The soft-mode behavior is similar to the one observed previously Ni-Al alloys [10], though phonon softening is much more pronounced in Ni_2MnGa. Figure 5 compares the temperature dependence of the TA_2 soft mode frequencies in Ni_2MnGa and $Ni_{62.5}Al_{37.5}$ [10]. $(\hbar\omega)^2$ decreases linearly with temperature in both materials, as T_M is approached. Note that it extrapolates to zero at T_0=250 K> T_M=220 K and T_0=-35 K << T_M = 80 K in Ni_2MnGa and $Ni_{62.5}Al_{37.5}$ respectively. At T_0 the original cubic lattice becomes *dynamically* unstable, and a premartensitic transition in Ni_2MnGa is bound to occur at $T_1 T_0 > T_M$. The fact that $T_1 > T_0$ indicates that the PM transition is of (weakly) 1st order. The nature of the lattice modulation in the PM phase suggests that the PM transition is *directly driven by the soft mode*. The fact that a second, martensitic transition occurs at still lower temperatures is a manifestation of strong *anharmonic coupling of the modulated strains to homogeneous lattice distortions* (the martensitic phase is described by both a tetragonal distortion of the lattice and a new periodic modulation in the $[1\ 1\ 0](1\ \bar{1}\ 0)$ system). This is supported by our recent inelastic neutron scattering studies of Ni2MnGa under uniaxial stress (these results will be published elsewhere). Such transformations may be adequately described by Landau- type theories developed by Krumhansl and Gooding [11]. We emphasize, that the superlattice wave vector in the martensitic phase is *different* from the soft phonon wave vector in the parent phase. The situation is similar to that in Ni-Al alloys and may be accounted for by the Landau theories mentioned above if the *Landau coefficients are allowed to be wave vector dependent* [10, 11].

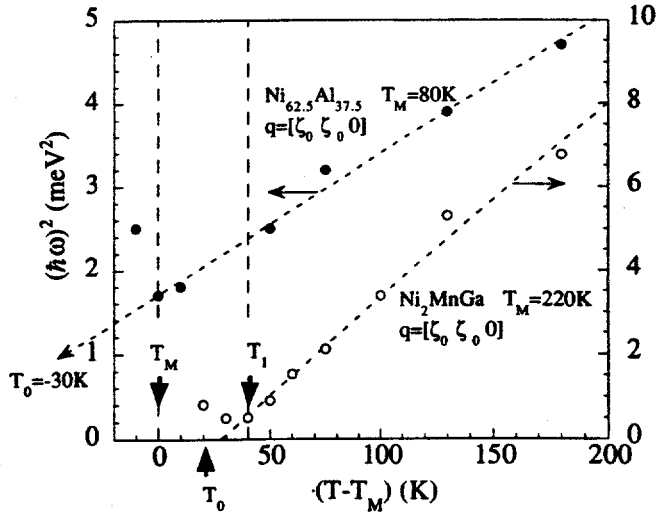

Figure 5: $(\hbar\omega)^2$ vs. T-T_M for the $[\zeta\ \zeta\ 0]$ TA_2 mode in Ni_2MnGa and $Ni_{62.6}Al_{37.5}$ (from Ref. [10]) in the point where the dispersion curve is a minimum.

Naturally, phenomenological theories are unable explain neither the origin of the phonon anomalies, nor their coupling to uniform strains. Showing that the "wiggle" in the TA_2 phonon dispersion curve in Ni_2MnGa persist above the ferromagnetic transition temperature, we have ruled out the possibility of relating the dispersion anomalies to phonon-magnon interaction, a mechanism which is active in several magnetically ordered systems[12]. It is generally agreed that the true origin of the phonon anomalies lies in *e-ph* coupling and specific nesting properties of the ``jungle-gym" Fermi surface [13,14]. The effect is similar to that produced by Kohn anomalies, but stems from the divergence in the *e-ph* matrix element, rather than in the dielectric susceptibility itself .

5. CONCLUSION.

A system undergoing a two-step martensitic phase transformation was studied by inelastic neutron scattering and electron microscopy. A strongly temperature-dependent anomaly in the TA_2 phonon dispersion observed in the parent cubic phase. The nearly complete softening of this mode at **q**=[1/3 1/3 0] results in a premartensitic first order phase transition which involves a modulated distortion of the parent structure with the same periodicity. Strong wave vector dependence of the coupling of periodic distortions to homogenous strains leads to a further transformation to an incommensurate martensitic phase at lower temperatures.

6. ACKNOWLEDGMENTS.

Work at Brookhaven National Laboratory was supported by the Division of Material Sciences, U. S. Department of Energy, under Contract No. DE-AC02-76CH00016. The work at Lawrence Livermore National Laboratory was performed under U. S. Department of Energy Contract No. W-7405-ENG-48.

[1] P. J. Webster, K. R. A. Ziebeck, S. L. Town, and M. S. Peak, *Philos. Mag.* **49** (1984) 295.
[2] V. V. Martynov and V. V. Kokorin, *J. Phys. III* (France) **2** (1992) 739.
[3] G. Fritsch, V. V. Kokorin, and A. Kempf, *J. Phys: Condens. Matter* **6** (1994) L107.
[4] V. A. Chernenko and V. V. Kokorin, in *Proceedings of the International Conference on Martensitic Transformations* (Monterey Institute for Advanced Sciences, Monterey, CA, USA, 1992), p. 1205; A. N. Vasil'ev, V. Kokorin, Y. I. Savchenko, and V. A. Chernenko, *Sov. Phys. JETP* **71** (1990) 803.
[5] J. D. Axe, S. M. Shapiro, G. Shirane, and T. riste, in *Anharmonic Lattice, Structural Transitions and Melting*, edited by T. riste (Nordhoff, Leiden, 1974).
[6] B. I. Halperin and C. M. Varma, *Phys. Rev. B* **14** (1976) 4030.
[7] L. E. Tanner, *Phylos. Mag.* **14** (1966), 111; L. E. Tanner, A. R. Pelton, and R. Gronsky, *J. Phys. (Paris) Colloq.* **43** (1982) C4; D. Schryvers and L. E. Tanner, *Ultramicroscopy* **37** (1990) 241.
[8] S. David, Master's thesis, CNRS, Laboratoire de Magnetisme Louis Neel, Grenoble, France, 1991.
[9] in *Structural Phase Transitions*, edited by A. D. Bruce and R. A. Cowley (Taylor and Francis, london, 1981).
[10] S. M. Shapiro *et al.*, *Phys. Rev. B* **44** (1991) 9301; S. M. Shapiro, E. C. Svensson, C. Vettier, and B. Hennion, *Phys. Rev. B* **48** (1993) 13223.
[11] R. J. Gooding and J. A. Krumhansl, *Phys, Rev. B* **39** (1989) 1535; J. A. Krumhansl and R. J. Gooding, *ibid.*, 3047; J. A. Krumhansl, *Solid State Comm.* **84** (1992) 251.
[12] See for example M. Sato, B. H. Grier, S. M. Shapiro, and H. Miyajima, *J. Phys. F: Met. Phys.* **12** (1982) 2117.
[13] C. M. Varma and W. Weber, *Phys. Rev B* **12** (1975) 2042.
[14] G. L. Zhao *et al.*, *Phys. Rev B* **43** (1989) 7999; G. L. Zhao and B. H. Harmon, *Phys. Rev. B* **45** (1992) 2818.